Published online July 7, 2005

Nucleic Acids Research, 2005, Vol. 33, No. 12 ***e107***
doi:10.1093/nar/gni107

A novel mammalian expression system derived from components coordinating nicotine degradation in *arthrobacter nicotinovorans* pAO1

Laetitia Malphettes[1], Cornelia C. Weber[2], Marie Daoud El-Baba[3], Ronald G. Schoenmakers[1,4], Dominique Aubel[3], Wilfried Weber[1] and Martin Fussenegger[1,*]

[1]Institute for Chemical and Bio-Engineering (ICB), Swiss Federal Institute of Technology, ETH Hoenggerberg, HCI F115, Wolfgang-Pauli-Strasse 10, CH-8093 Zurich, Switzerland, [2]Novartis Pharma AG, CH-4002 Basel, Switzerland, [3]Département Génie Biologique, Institut Universitaire de Technologie, IUTA, 43 Boulevard du 11 Novembre 1918, F-69622 Villeurbanne Cedex, France and [4]Integrative Bioscience Institute, Swiss Federal Institute of Technology Lausanne, CH-1015 Lausanne, Switzerland

Received March 29, 2005; Revised and Accepted June 20, 2005

ABSTRACT

We describe the design and detailed characterization of 6-hydroxy-nicotine (6HNic)-adjustable transgene expression (NICE) systems engineered for lentiviral transduction and *in vivo* modulation of angiogenic responses. *Arthrobacter nicotinovorans* pAO1 encodes a unique catabolic machinery on its plasmid pAO1, which enables this Gram-positive soil bacterium to use the tobacco alkaloid nicotine as the exclusive carbon source. The 6HNic-responsive repressor-operator (HdnoR-O_{NIC}) interaction, controlling 6HNic oxidase production in *A.nicotinovorans* pAO1, was engineered for generic 6HNic-adjustable transgene expression in mammalian cells. HdnoR fused to different transactivation domains retained its O_{NIC}-binding capacity in mammalian cells and reversibly adjusted transgene transcription from chimeric O_{NIC}-containing promoters (P_{NIC}; O_{NIC} fused to a minimal eukaryotic promoter [P_{min}]) in a 6HNic-responsive manner. The combination of transactivators containing various transactivation domains with promoters differing in the number of operator modules as well as in their relative inter-O_{NIC} and/or O_{NIC}-P_{min} spacing revealed steric constraints influencing overall NICE regulation performance in mammalian cells. Mice implanted with microencapsulated cells engineered for NICE-controlled expression of the human glycoprotein secreted placental alkaline phosphatase (SEAP) showed high SEAP serum levels in the absence of regulating 6HNic. 6HNic was unable to modulate SEAP expression, suggesting that this nicotine derivative exhibits control-incompatible pharmacokinetics in mice. However, chicken embryos transduced with HIV-1-derived self-inactivating lentiviral particles transgenic for NICE-adjustable expression of the human vascular endothelial growth factor 121 ($VEGF_{121}$) showed graded 6HNic response following administration of different 6HNic concentrations. Owing to the clinically inert and highly water-soluble compound 6HNic, NICE-adjustable transgene control systems may become a welcome alternative to available drug-responsive homologs in basic research, therapeutic cell engineering and biopharmaceutical manufacturing.

INTRODUCTION

The Gram-positive soil bacterium *Arthrobacter nicotinovorans* pAO1 acquired the metabolic capacity to metabolize the tobacco alkaloid nicotine as an exclusive carbon source. Utilization is initiated by hydroxylation of nicotine's pyridine ring at position C6 followed by oxidation mediated by the 6-hydroxy-nicotine oxidase (6HNO). Recent sequence analysis of the catabolic plasmid pAO1 revealed the 6HNO gene repressor HdnoR, which controls 6HNO expression in the presence of 6-hydroxy-nicotine (6HNic) (1). 6HNic modulates HdnoR's allosteric conformation in a way that prevents further binding and repression of the 6HNO promoter, thereby resulting in induction of follow-up nicotine-specific metabolic

*To whom correspondence should be addressed. Tel: +41 44 633 3448; Fax: +41 44 633 1234; Email: fussenegger@chem.ethz.ch

pathways. 6HNic produced by *A.nicotinovorans* pAO1 came into the limelight as a bio-catalytic bulk product, which can be employed in conventional esterification processes or as an educt for the production of particular special chemicals, including 6-alkoxynicotine derivatives known to exhibit antibacterial and antifungal activities (2). In addition to being an intermediate product in (bio-) chemical production scenarios, 6HNic is also a by-product of pioneering efforts to denicotinize tobacco for the production of 'mild' or 'light' cigarettes characterized by a low nicotine content (3,4). Besides its involvement in the aforementioned processes, knowledge of 6HNic's physiologic impact and pharmacokinetics is limited or non-existing. However, unlike nicotine itself, 6HNic is expected to be more soluble and unable to trigger nicotine-specific receptor responses because of its hydroxylated aromatic ring (5).

HdnoR has been reported to belong to the TetR family of bacterial response regulators, which repress target genes in a physiologic compound-responsive manner (1). In particular, TetR dissociates from a cognate P_{TetA} promoter in the presence of tetracycline antibiotics and so induces the expression of the tetracycline resistance gene *tetA* (6). Pioneering efforts in using bacterial response regulators for mammalian transgene expression fine-tuning have resulted in the design of the tetracycline-responsive expression system [the TET system(s)], which consists of its generic configuration of TetR fused to a *Herpes simplex*-derived VP16 transactivation domain (tTA) and a heptameric TetR-specific *tetA* promoter-derived operator module (*tetO*$_7$) functionally linked to the minimal version of the human cytomegalovirus immediate early promoter (*tetO*$_7$-$P_{hCMVmin}$; $P_{hCMV*-1}$). tTA binding to $P_{hCMV*-1}$ induced desired transgene transcription in the absence of tetracycline. However, tetracycline switched tTA's allosteric conformation to a $P_{hCMV*-1}$ binding-incompetent state, which resulted in dose-dependent transgene repression (7).

Following the generic design principle of the TET system, a wide variety of bacterial response regulators have been adapted for use as mammalian gene regulation systems, including those responsive to (i) tetracycline derivatives (7,8), (ii) streptogramin (9), (iii) macrolide (10) and (iv) coumermycin (11) antibiotics, (v) immunosuppressive rapamycin (12), hormones such as (vi) estrogen (13), (vii) progesterone (14) and (viii) ecdysone (15), (ix) temperature (16), (x) quorum-sensing molecules (17,18), (xi) the terpene cumate (http://www.qbiogene.com/products/gene-expression/qmateslideshow/index.htm), (xii) the type-2 diabetes drug roziglitazone (19) and (xiii) gaseous acetaldehyde (20).

Most transgene regulation modalities were conceived or have been used as stand-alone systems [one-gene control system modulating a single (set of) transgene(s)] for targeted molecular interventions in complex regulatory networks, including (i) prototype gene therapy and tissue engineering scenarios (12,21), (ii) drug discovery (22,23), (iii) biopharmaceutical manufacturing (24,25) and (iv) gene-function analysis (26). Clinically licensed antibiotics (macrolide, streptogramin, coumermycin and tetracycline), immunosuppressive agents (rapamycin), hormones (mifepristone) and PPAR-γ (peroxisome proliferator-activated receptor-γ) agonists (roziglitazone) seem to be ideal candidates for gene therapy-based conditional transgene interventions. However, some of these drugs may elicit side effects following long-term administration at regulation-effective concentrations (27–29). Furthermore, drug-based inducers are less suited for transgene modulation of biotechnologically relevant production cell lines, since preparation of inducer-free product formulations remains a costly downstream processing challenge.

Availability of different compatible transgene regulation systems enabled their functional interconnection to produce synthetic mammalian networks with unprecedented signal integration. The most prominent mammalian cell-embedded synthetic regulatory networks include: (i) an artificial regulatory cascade consisting of three heterologous transcription control units interconnected in a linear manner to produce discrete multilevel expression control of a terminally encoded transgene in response to clinical doses of different antibiotics (30), (ii) an epigenetic circuitry able to switch between two stable transgene expression states after transient administration of two alternate drugs (31) and BioLogic gates providing transgene expression integration reminiscent of digital electronics (32).

We have designed a novel gene regulation system [6HNic-adjustable transgene expression (NICE)] responsive to the non-toxic nicotine derivative 6HNic. NICE technology enabled fine-tuning of transgene expression in mammalian cells, was compatible with state-of-the-art lentiviral transduction and provided precise control of angiogenic responses in chicken embryos. Since NICE systems are responsive to a clinically inert, highly water-soluble nicotine derivative, we believe it will foster advances in basic research as well as in biopharmaceutical manufacturing.

MATERIALS AND METHODS

Plasmid construction

All plasmids used in this study are listed in Table 1; detailed information on their construction is also provided.

Cell culture and transfection

Chinese hamster ovary cells (CHO-K1, ATCC CCL 61) were cultivated in standard medium: FMX-8 medium (Cell Culture Technologies, Zurich, Switzerland) supplemented with 10% fetal calf serum (FCS) (Pan Biotech GmbH, Aidenbach, Germany; catalog no. 3302-P231902, lot no. P231902). Human embryonic kidney cells transgenic for simian virus 40 (SV40) large T antigen [HEK293-T (33)] were cultivated in DMEM (Invitrogen, Carlsbad, CA) supplemented with 10% FCS. All cell lines were cultivated at 37°C in a 5% CO_2-containing humidified atmosphere. CHO-K1 cells were transfected using an optimized calcium phosphate-based protocol that resulted in standard transfection efficiencies of 35 ± 5%. In brief, 40 000 CHO-K1 cells were seeded per well of a 24-well plate and cultivated overnight. Aliquots containing 6 μg of plasmid DNA (for cotransfections equal amounts of each plasmid were used) were diluted in 60 μl of 250 mM $CaCl_2$ and precipitated following drop-wise addition of 60 μl phosphate solution for 20 s (50 mM HEPES, 280 mM NaCl, 1.5 mM Na_2HPO_4, pH 7.1). Following further incubation for 10 s, 2 ml FMX-8 containing 2% FCS were added. The culture medium was replaced by the DNA-precipitate-containing

Table 1. Plasmids used and designed in this study

Plasmid	Description and cloning strategy	Reference or source
pBM57	HIV-1-derived lentiviral expression vector (5′LTR-ψ^+-ori$_{SV40}$-cPPT-RRE-EYFP-3′LTR$_{\Delta U3}$)	(33)
pBM104	Lentiviral expression vector encoding a P_{PIR8}-driven $VEGF_{121}$ expression unit (5′LTR-ψ^+-ori$_{SV40}$-cPPT-RRE-P_{PIR8}-$VEGF_{121}$-3′LTR$_{\Delta U3}$)	(68)
pBM105	Lentiviral expression vector encoding a P_{PIR8}-driven SEAP expression unit (5′LTR-ψ^+-ori$_{SV40}$-cPPT-RRE-P_{PIR8}-$VEGF_{121}$-3′LTR$_{\Delta U3}$)	(68)
pBP10	Vector encoding a P_{ETR5}-driven SEAP expression unit (P_{ETR5}-SEAP-pA; P_{ETR5}, ETR-2bp-$P_{hCMVmin}$)	(47)
pBP11	Vector encoding a P_{ETR6}-driven SEAP expression unit (P_{ETR6}-SEAP-pA; P_{ETR6}, ETR-4bp-$P_{hCMVmin}$)	(47)
pBP12	Vector encoding a P_{ETR7}-driven SEAP expression unit (P_{ETR7}-SEAP-pA; P_{ETR7}, ETR-6bp-$P_{hCMVmin}$)	(47)
pBP13	Vector encoding a P_{ETR8}-driven SEAP expression unit (P_{ETR8}-SEAP-pA; P_{ETR8}, ETR-8bp-$P_{hCMVmin}$)	(47)
pBP14	Vector encoding a P_{ETR9}-driven SEAP expression unit (P_{ETR9}-SEAP-pA; P_{ETR9}, ETR-10bp-$P_{hCMVmin}$)	(47)
pH6EX3-HdnoR	Vector encoding the *A.nicotinovorans* pAO16 repressor of the 6HNic oxidase (HdnoR)	(1)
pLM82	Constitutive NT1 expression vector (P_{SV40}-NT1-pA; NT1, HdnoR-VP16) HdnoR was PCR-amplified from pH6EX3-HdnoR using OLM83: 5-*GTACgaattcCCACC*atgcgtatttccacggtggatcg-3′ and OLM84: 5′-*CTTATGgcgcgcGGCTGTACGCGGA*tagtcctacccgatcgaggta-3′ (lower case, annealing sequence; lower case italics, restriction sites), restricted with EcoRI/BssHII and ligated into the corresponding sites (EcoRI/BssHII) of pWW35	This work
pLM83	Vector encoding a P_{NIC1a}-driven SEAP expression unit (P_{NIC1a}-SEAP-pA; P_{NIC1a}, O_{NIC}-0bp-$P_{hCMVmin}$) $P_{hCMVmin}$ was PCR-amplified from pRevTRE using OLM82: 5′-*GATCgacgtc*CCCCATTGACATGGACAGCTGTC-CATGTATCAATAGGGTG*cctgcagg*tcgagctcggtacccgggtc-3′ and OWW22: 5′-*GCTAgaattc*cgcggaggctggatcgg-3′ (lower case, annealing sequence; lower case italics, restriction sites; upper case, O_{NIC}), restricted with AatII/EcoRI and ligated into the corresponding sites (AatII/EcoRI) of pMF111	This work
pLM101	Constitutive NT2 expression vector (P_{SV40}-NT2-pA; NT2, HdnoR-p65) The NF-κB-derived transactivation domain (p65) was excised from pWW42 using BssHII/BamHI and ligated into the corresponding sites (BssHII/BamHI) of pLM82	This work
pLM102	Constitutive NT3 expression vector (P_{SV40}-NT3-pA; NT3, HdnoR-E2F4) The E2F4-derived transactivation domain (E2F4) was excised from pWW64 using BssHII/BamHI and ligated into the corresponding sites (BssHII/BamHI) of pLM82	This work
pLM103	Lentiviral NT1 expression vector (5′LTR-ψ^+-ori$_{SV40}$-cPPT-RRE-$P_{hEF1\alpha}$-NT1-3′LTR$_{\Delta U3}$; NT1, HdnoR-VP16) NT1 was excised from pLM82 using NotI/XmaI and ligated into the corresponding sites (NotI/XmaI) of pMF391	This work
pLM104	Vector encoding a P_{NIC1b}-driven SEAP expression unit (P_{NIC1b}-SEAP-pA; P_{NIC1b}, O_{NIC}-2bp-$P_{hCMVmin}$) 2bp-$P_{hCMVmin}$-SEAP was excised from pBP10 using SbfI/XhoI and ligated into the corresponding sites (SbfI/XhoI) of pLM83	This work
pLM105	Vector encoding a P_{NIC1c}-driven SEAP expression unit (P_{NIC1c}-SEAP-pA; P_{NIC1c}, O_{NIC}-4bp-$P_{hCMVmin}$) 4bp-$P_{hCMVmin}$-SEAP was excised from pBP11 using SbfI/XhoI and ligated into the corresponding sites (SbfI/XhoI) of pLM83	This work
pLM106	Vector encoding a P_{NIC1d}-driven SEAP expression unit (P_{NIC1d}-SEAP-pA; P_{NIC1d}, O_{NIC}-6bp-$P_{hCMVmin}$) 6bp-$P_{hCMVmin}$-SEAP was excised from pBP12 using SbfI/XhoI and ligated into the corresponding (SbfI/XhoI) sites of pLM83	This work
pLM107	Vector encoding a P_{NIC1e}-driven SEAP expression unit (P_{NIC1e}-SEAP-pA; P_{NIC1e}, O_{NIC}-8bp-$P_{hCMVmin}$) 8bp-$P_{hCMVmin}$-SEAP was excised from pBP13 using SbfI/XhoI and ligated into the corresponding (SbfI/XhoI) sites of pLM83	This work
pLM108	Vector encoding a P_{NIC1f}-driven SEAP expression unit (P_{NIC1f}-SEAP-pA; P_{NIC1f}, O_{NIC}-10bp-$P_{hCMVmin}$) 10bp-$P_{hCMVmin}$-SEAP was excised from pBP14 using SbfI/XhoI and ligated into the corresponding (SbfI/XhoI) sites of pLM83	This work
pLM116	BamHI-AscI-StuI-AatII-XbaI-ONIC-0bp-NheI-SbfI-EcoRI-EPO was PCR-amplified from pWW139 using OLM90 5′-CGggatccAggcgcgccAaggcctTTgacgtctctagaTACCCCATTGACATGGACAGCTGTCCATGTATCAA-TAGGGTGTgctagcTTcctgcagggaattccaccatgg-3′ and OWW51 5′-gcgcgcatcgattcacctgtcccctctcctgcag-3′, restricted with (BamHI/ClaI) and ligated into the corresponding sites (BamHI/ClaI) of pWW139 (lower case, annealing sequence; lower case italics, restriction sites; upper case, O_{NIC})	This work
pLM118	O_{NIC}-NheI-SbfI-EcoRI-EPO was excised from pLM116 using XbaI/ClaI and ligated into the compatible sites (XbaI/ClaI) of pLM116. $P_{hEF1\alpha}$-O_{NIC2}-0bp-O_{NIC1}-EPO-pA	This work
pLM119	AscI-StuI-AatII-XbaI-O_{NIC}-2bp-NheI-SbfI-EcoRI-EPO was PCR-amplified from pWW139 using OLM91 5′-CGggatccAggcgcgccAaggcctTTgacgtctctagaTACCCCATTGACATGGACAGCTGTCCATGTATCAAT-AGGGTGATTgctagcTTcctgcagggaattccaccatgg-3′ and OWW51 5′-gcgcgcatcgattcacctgtcccctctcctgcag-3′, restricted with AscI/ClaI and ligated into the corresponding sites (AscI/ClaI) of pLM116. $P_{hEF1\alpha}$-O_{NIC2}-2bp-O_{NIC1}-EPO-pA	This work
pLM120	AscI-StuI-AatII-XbaI-O_{NIC}-4bp-NheI-SbfI-EcoRI-EPO was PCR-amplified from pWW139 using OLM92 5′-CGggatccAggcgcgccAaggcctTTgacgtctctagaTACCCCATTGACATGGACAGCTGTCCATGTATCAA-TAGGGTGATCGTgctagcTTcctgcagggaattccaccatgg-3′ and OWW51 5′-gcgcgcatcgattcacctgtcccctctcctgcag-3′, restricted with AscI/ClaI and ligated into the corresponding sites (AscI/ClaI) of pLM116. $P_{hEF1\alpha}$-O_{NIC2}-4bp-O_{NIC1}-EPO-pA	This work
pLM121	AscI-StuI-AatII-XbaI-O_{NIC}-6bp-NheI-SbfI-EcoRI-EPO was PCR-amplified from pWW139 using OLM93 5′-CGggatccAggcgcgccAaggcctTTgacgtctctagaTACCCCATTGACATGGACAGCTGTCCATGTATCAAT-AGGGTGATCGTATgctagcTTcctgcagggaattccaccatgg-3′ and OWW51 5′-gcgcgcatcgattcacctgtcccctctcctgcag-3′, restricted with AscI/ClaI and ligated into the corresponding sites (AscI/ClaI) of pLM116. $P_{hEF1\alpha}$-O_{NIC2}-6bp-O_{NIC1}-EPO-pA	This work
pLM122	AscI-StuI-AatII-XbaI-O_{NIC}-8bp-NheI-SbfI-EcoRI-EPO was PCR-amplified from pWW139 using OLM94 5′-CGggatccAggcgcgccAaggcctTTgacgtctctagaTACCCCATTGACATGGACAGCTGTCCATGTATCAATAG-GGTGATCGTAATTgctagcTTcctgcagggaattccaccatgg-3′ and OWW51 5′-gcgcgcatcgattcacctgtcccctctcctgcag-3′, restricted with AscI/ClaI and ligated into the corresponding sites (AscI/ClaI) of pLM116. $P_{hEF1\alpha}$-O_{NIC2}-8bp-O_{NIC1}-EPO-pA	This work

Table 1. *Continued*

Plasmid	Description and cloning strategy	Reference or source
pLM123	AscI-StuI-AatII-XbaI-O_{NIC}-10bp-NheI-SbfI-EcoRI-EPO was PCR-amplified from pWW139 using OLM95 5′-CGggatccAggcgcgccAaggcctTTgacgtctctagaTACCCCATTGACATGGACAGCTGTCCATGTATCAATAGG-GTGATCGTACGATTgctagcTTcctgcagggaattccaccatgg-3′ and OWW51 5′-gcgcgcatcgattcacctgtcccctctcctgcag-3′, restricted with AscI/ClaI and ligated into the corresponding sites (AscI/ClaI) of pLM116. $P_{hEF1\alpha}$-O_{NIC2}-10bp-O_{NIC1}-EPO-pA	This work
pLM124	O_{NIC}-NheI-SbfI-EcoRI-EPO was excised from pLM116 using XbaI/ClaI and ligated into the compatible sites (NheI/ClaI) of pLM119, thereby resulting in P_{hCMV}-O_{NIC2}-2bp-O_{NIC1}-EPO-pA	This work
pLM125	O_{NIC}-NheI-SbfI-EcoRI-EPO was excised from pLM116 using XbaI/ClaI and ligated into the compatible sites (NheI/ClaI) of pLM120, thereby resulting in P_{hCMV}-O_{NIC2}-4bp-O_{NIC1}-EPO-pA	This work
pLM126	O_{NIC}-NheI-SbfI-EcoRI-EPO was excised from pLM116 using XbaI/ClaI and ligated into the compatible sites (NheI/ClaI) of pLM121, thereby resulting in P_{hCMV}-O_{NIC2}-6bp-O_{NIC1}-EPO-pA	This work
pLM127	O_{NIC}-NheI-SbfI-EcoRI-EPO was excised from pLM116 using XbaI/ClaI and ligated into the compatible sites (NheI/ClaI) of pLM122, thereby resulting in P_{hCMV}-O_{NIC2}-8bp-O_{NIC1}-EPO-pA	This work
pLM128	O_{NIC}-NheI-SbfI-EcoRI-EPO was excised from pLM116 using XbaI/ClaI and ligated into the compatible sites (NheI/ClaI) of pLM123, thereby resulting in P_{hCMV}-O_{NIC2}-10bp-O_{NIC1}-EPO-pA	This work
pLM129	P_{hCMV}-O_{NIC2}-0bp-O_{NIC1}-NheI was excised from pLM118 using ScaI/SbfI and ligated into the corresponding sites (ScaI/SbfI) of pLM105, thereby resulting in P_{hCMV}-O_{NIC2}-0bp-O_{NIC1}-NheI-SbfI-4bp-$P_{hCMVmin}$-SEAP-pA	This work
pLM130	P_{hCMV}-O_{NIC2}-2bp-O_{NIC1} was excised from pLM124 using ScaI/SbfI and ligated into the corresponding sites (ScaI/SbfI) of pLM105, thereby resulting in P_{hCMV}-O_{NIC2}-2bp-O_{NIC1}-NheI-SbfI-4bp-$P_{hCMVmin}$-SEAP-pA	This work
pLM131	P_{hCMV}-O_{NIC2}-4bp-O_{NIC1} was excised from pLM125 using ScaI/SbfI and ligated into the corresponding sites (ScaI/SbfI) of pLM105, thereby resulting in P_{hCMV}-O_{NIC2}-4bp-O_{NIC1}-NheI-SbfI-4bp-$P_{hCMVmin}$-SEAP-pA	This work
pLM132	P_{hCMV}-O_{NIC2}-6bp-O_{NIC1} was excised from pLM126 using ScaI/SbfI and ligated into the corresponding sites (ScaI/SbfI) of pLM105, thereby resulting in P_{hCMV}-O_{NIC2}-6bp-O_{NIC1}-NheI-SbfI-4bp-$P_{hCMVmin}$-SEAP-pA	This work
pLM133	P_{hCMV}-O_{NIC2}-8bp-O_{NIC1} was excised from pLM127 using ScaI/SbfI and ligated into the corresponding sites (ScaI/SbfI) of pLM105, thereby resulting in P_{hCMV}-O_{NIC2}-8bp-O_{NIC1}-NheI-SbfI-4bp-$P_{hCMVmin}$-SEAP-pA	This work
pLM134	P_{hCMV}-O_{NIC2}-10bp-O_{NIC1} was excised from pLM128 using ScaI/SbfI and ligated into the corresponding sites (ScaI/SbfI) of pLM105, thereby resulting in P_{hCMV}-O_{NIC2}-10bp-O_{NIC1}-NheI-SbfI-4bp-$P_{hCMVmin}$-SEAP-pA	This work
pLM135	Vector encoding a P_{NIC2a}-driven SEAP expression unit (P_{NIC2a}-SEAP-pA; P_{NIC2a}, O_{NIC2}-0bp-O_{NIC1}-NheI-SbfI-4bp-$P_{hCMVmin}$). P_{hCMV} was excised from pLM129 using AatII/AatII and the pLM129 backbone was self-ligated	This work
pLM136	Vector encoding a P_{NIC2b}-driven SEAP expression unit (P_{NIC2b}-SEAP-pA; P_{NIC2b}, O_{NIC2}-2bp-O_{NIC1}-NheI-SbfI-4bp-$P_{hCMVmin}$). P_{hCMV} was excised from pLM130 using AatII/AatII and the pLM130 backbone was self-ligated	This work
pLM137	Vector encoding a P_{NIC2c}-driven SEAP expression unit (P_{NIC2c}-SEAP-pA; P_{NIC2c}, O_{NIC2}-4bp-O_{NIC1}-NheI-SbfI-4bp-$P_{hCMVmin}$). P_{hCMV} was excised from pLM131 using AatII/AatII and the pLM131 backbone was self-ligated	This work
pLM138	Vector encoding a P_{NIC2d}-driven SEAP expression unit (P_{NIC2d}-SEAP-pA; P_{NIC2d}, O_{NIC2}-6bp-O_{NIC1}-NheI-SbfI-4bp-$P_{hCMVmin}$). P_{hCMV} was excised from pLM132 using AatII/AatII and the pLM132 backbone was self-ligated	This work
pLM139	Vector encoding a P_{NIC2e}-driven SEAP expression unit (P_{NIC2e}-SEAP-pA; P_{NIC2e}, O_{NIC2}-8bp-O_{NIC1}-NheI-SbfI-4bp-$P_{hCMVmin}$). P_{hCMV} was excised from pLM133 using AatII/AatII and the pLM133 backbone was self-ligated	This work
pLM140	Vector encoding a P_{NIC2f}-driven SEAP expression unit (P_{NIC2f}-SEAP-pA; P_{NIC2f}, O_{NIC2}-10bp-O_{NIC1}-NheI-SbfI-4bp-$P_{hCMVmin}$). P_{hCMV} was excised from pLM134 using AatII/AatII and the pLM134 backbone was self-ligated	This work
pLM141	P_{NIC2d} (O_{NIC2}-6bp-O_{NIC1}-NheI-SbfI-4bp-$P_{hCMVmin}$) was excised from pLM132 (AscI/EcoRI) and ligated into the corresponding sites (AscI/EcoRI) of pBM105 (5′LTR-ψ^+-oriSV40-cPPT-RRE-P_{NIC2d}-SEAP-3′$LTR_{\Delta U3}$; P_{NIC2d}, O_{NIC2}-6bp-O_{NIC1}-NheI-SbfI-4bp-$P_{hCMVmin}$)	This work
pLM145	$P_{hCMVmin}$-$VEGF_{121}$ was excised from pBM104 using SbfI/SspI and ligated into the corresponding sites (SbfI/SspI) of pLM120, thereby resulting in P_{NIC3}-$VEGF_{121}$-pA (P_{NIC3}, O_{NIC}-4bp-NheI-SbfI-$P_{hCMVmin}$)	This work
pLM146	Lentiviral expression vector encoding a P_{NIC3}-driven $VEGF_{121}$ expression unit (5′LTR-ψ^+-ori_{SV40}-cPPT-RRE-P_{NIC3}-$VEGF_{121}$-3′$LTR_{\Delta U3}$; P_{NIC3}, O_{NIC}-4bp-NheI-SbfI-$P_{hCMVmin}$). P_{NIC3}–$VEGF_{121}$ was excised from pLM145 using AscI/MluI and ligated into the corresponding sites (AscI/MluI) of pBM104	This work
pMF111	Vector encoding a P_{hCMV^*-1}-driven SEAP expression unit (P_{hCMV^*-1}-SEAP-pA)	(69)
pMF391	Lentiviral ET1 expression vector (5′LTR-ψ^+-ori_{SV40}-PPT-RRE- $P_{hEF1\alpha}$-ET1-3′$LTR_{\Delta U3}$)	(70)
pRevTRE	Oncoretroviral expression vector containing a tetracycline-responsive expression unit	Clontech, Palo Alto, CA
Pseap2-Control	Constitutive P_{SV40}-driven SEAP expression vector	Clontech, Palo Alto, CA
pWW35	Constitutive ET1 expression vector (P_{SV40}-ET1-pA)	(10)
pWW42	Constitutive ET2 expression vector (P_{SV40}-ET2-pA)	(10)
pWW64	Constitutive ET4 expression vector (P_{SV40}-ET4-pA)	(10)
pWW139	EPO expression vector	(18)

3′$LTR_{\Delta U3}$, enhancer-free 3′ long terminal repeat; 5′LTR, 5′ long terminal repeat; 6HNic, 6-hydroxy-nicotine; cPPT, central polypurine tract; E2F4, human transcription factor, transactivation domain of the human E2F4; EPO, erythropoetin; ET1, macrolide-dependent transactivator (MphR(A)-VP16); ET2, macrolide-dependent transactivator (MphR(A)-p65); ET4, macrolide-dependent transactivator (MphR(A)-E2F4); ETR, operator module specific for MphR(A); EYFP, enhanced yellow fluorescent protein; HdnoR, repressor of the *A.nicotinovorans* pAO1 6HNic oxidase gene; MphR(A), *E.coli*-derived repressor of the macrolide resistance gene *mphA*; NF-κB, human transcription factor; NT1, 6HNic-dependent transactivator (HdnoR-VP16); NT2, 6HNic-dependent transactivator (HdnoR-p65); NT3, 6HNic-dependent transactivator (HdnoR-E2F4); O_{NIC}, HdnoR-specific operator; $O_{NIC1/2}$, O_{NIC} numbering in tandem operator configurations; ori_{SV40}, origin of replication of the SV40; p65, transactivation domain of NF-κB; pA; SV40-derived polyadenylation site; P_{ETR2}, macrolide-responsive promoter (ETR-$P_{hCMVmin}$); $P_{ETR5\text{-}9}$, macrolide-responsive promoters containing different spacers between ETR and $P_{hCMVmin}$; P_{hCMV}, promoter of the human cytomegalovirus immediate early promoter; $P_{hCMVmin}$, minimal P_{hCMV}; P_{hCMV^*-1}, tetracycline-responsive promoter; $P_{hEF1\alpha}$, promoter of the human elongation factor 1 alpha; $P_{NIC1a\text{-}f}$, 6HNic-responsive promoters containing different spacers between O_{NIC} and $P_{hCMVmin}$; $P_{NIC2a\text{-}f}$, 6HNic-responsive promoters containing tandem O_{NIC} operators with different inter-O_{NIC} spacing but fixed spacing relative to $P_{hCMVmin}$; P_{NIC3}, 6HNic-responsive promoter with extended spacing between O_{NIC} and $P_{hCMVmin}$; P_{PIR8}, streptogramin-dependent promoter; P_{SV40}, constitutive SV40 promoter; RRE, rev response element; SEAP, human placental secreted alkaline phosphatase; $VEGF_{121}$, human vascular endothelial growth factor 121; VP16, *H.simplex* virus-derived transactivation domain; ψ^+, extended lentiviral packaging signal.

medium and incubated for 5 h prior to a glycerol shock for 30 s (FMX-8 medium supplemented with 15% glycerol and 2% FCS). After a single washing step using standard medium, cells were cultivated for analysis in the presence or absence of regulating 6HNic (50 μg/ml, unless stated otherwise). Forty-eight hours post glycerol shock, reporter protein expression was profiled.

Lentiviral particle production and transduction

For production of replication-incompetent self-inactivating HIV-1-derived lentiviral particles, HEK293-T cells were co-transfected following an optimized calcium phosphate-based protocol. In brief, 200 000 HEK293-T cells were seeded per well of a 6-well plate and cultivated overnight in 2 ml 10% FCS-containing DMEM. For each transfection, 1 μg pLTR-G [encoding the pseudotyping envelope protein VSV-G of the vesicular stomatitis virus (34)], 1 μg pCD/NL-BH* [helper construct (35)] and 1 μg of the desired transgene-encoding lentiviral expression vector were diluted in 100 μl of 250 mM $CaCl_2$. The DNA mixture was added drop-wise to 100 μl phosphate solution (100 mM HEPES, 280 mM NaCl, 1.5 mM Na_2HPO_4, pH 7.1), incubated for 15 min to enable formation of DNA-$CaPO_4$ precipitates, which were subsequently added to HEK293-T cultures. Five-hours post-transfection, the DNA–$CaPO_4$ complex was removed by medium exchange and lentiviral particles were produced for another 48 h prior to collection from the supernatant by filtration through a 0.45 μm filter (PIR8FP 030/2; Schleicher & Schuell GmbH, Dassel, Germany). This protocol typically yielded lentiviral particle titers of 2×10^7 c.f.u./ml following titration on CHO-K1 cells or enzyme-linked immunosorbent assay-based p24 quantification according to the manufacturer's protocol (catalog no. 103; Immunodiagnostics Inc., Woburn, MA). In order to prevent cross-contamination of secreted proteins from production supernatants and increase overall transduction efficiency, lentiviral particles were concentrated by ultracentrifugation for 2 h at 43 000 *g* and 4°C (Beckman Quick-Seal centrifuge tubes; catalog no. 342413, Beckman Instruments Inc., CA). The pellets were resuspended in 10% FCS-containing DMEM to adjust viral concentrations to desired levels. Furthermore, the culture medium was exchanged 6 h post transduction to ensure that transgene expression was exclusively based on transduction. Unless stated otherwise, standard transduction experiments included infection of 24 000 target cells seeded per well of a 12-well plate with 8×10^5 c.f.u. lentiviral particles (4 ng of p24).

Quantification of reporter protein production

Product proteins were quantified in cell culture supernatants 48 h after transduction. Human placental secreted alkaline phosphatase (SEAP) production was assessed using a chemiluminescence-based assay (Roche Diagnostics AG, Rotkreuz, Switzerland). Human vascular endothelial growth factor 121 ($VEGF_{121}$) production was quantified using the human VEGF-specific DuoSet ELISA System (R&D Systems, Minneapolis, MO) according to the manufacturer's protocol.

In vivo methods I—mice

CHO-K1 cells engineered for NICE-controlled SEAP expression by cotransfection of pLM82 (P_{SV40}-NT1-pA) and pLM104 (P_{NIC1b}-SEAP-pA) were encapsulated in coherent alginate-poly-(L-lysine)-alginate beads (200 cells/capsule, 2×10^6 cells/mouse) as described previously (10) and implanted intraperitoneally into female OF1 mice (oncins France souche 1; Iffa-Credo, Lyon, France). At 1 h after capsule implantation, 6HNic was administered by intraperitoneal injection at doses ranging from 0 to 100 mg/kg. 6HNic was formulated for *in vivo* administration by dilution of stock solutions to appropriate concentrations using physiological salt solution [0.9% (w/v); Laboratoire Aguettant, Lyon, France]. Control mice harbored encapsulated wild-type CHO-K1 cells. At 72 h after 6HNic administration, the mice were killed for blood collection and quantification of SEAP serum levels using microtainer SST tubes (Beckton Dickinson, Plymouth, UK) according to the manufacturer's protocol. All experiments involving mice were approved by the French Ministry of Agriculture and Fishery (Paris, France) and performed by M. D. El-Baba at the Institut Universitaire de Technologie, IUTA, F-69622 Villeurbanne Cedex, France.

In vivo methods II—transduction of chicken embryos

The shell-free cultivation protocols of Djonov and co-workers (36) were used for all experiments involving chicken embryos. Brown Leghorn eggs were opened after 3 days incubation at 37°C and their contents were carefully poured into 80 mm plastic Petri dishes. The chicken embryos were incubated at 37°C in a humidified atmosphere. On embryonic day 9, pLM146- (100 μl in DMEM, 8.5×10^6 c.f.u., 40 ng p24) and pLM103- (90 μl in DMEM, 6.4×10^5 c.f.u., 3 ng p24) derived lentiviral particles were co-applied locally on top of the growing chorioallantoic membrane (CAM) together with 0.5 μl (0.5 nM in DMEM) CellTracker orange CMTMR (catalog no. C-2927; Molecular Probes Inc., Eugene, OR) to tag the transduction site. In order to modulate heterologous $VEGF_{121}$ expression, different concentrations of 6HNic (0, 0.1, 1 and 50 μg/ml) were administered 1 h post transduction. On embryonic day 12, the CAMs were examined by *in vivo* fluorescence microscopy following intravenous injection of 100 μl 2.5% fluoresceine isothiocyanate dextran (FITC) (2 000 000; Sigma Chemicals, St Louis, MO) (37). FITC-stained CAM blood vessels were visualized at 50× and 100× magnifications using a Leica DM-RB fluorescence microscope equipped with a Leica digital fluorescence camera DC300 FX (Leica Microsystems AG, Heerbrugg, Switzerland) and a XF114 filter (Omega Optical Inc., Brattleboro, VT).

HPLC-based quantification of 6-hydroxy-nicotine

6HNic concentrations in 2 μl mouse urine samples were quantified by high-performance liquid chromatography (HPLC) [reversed-phase C18 column (Atlantis®C18, 4.6 × 150 mm; Waters Associates Inc.), Waters 2695 Separation Module (Waters Associates Inc.), Waters 996 Photodiode Array Detector (Waters Associates Inc.)]. Using an isocratic elution system of 0.1% TFA in water/acetonitrile (98:2 v/v) at a flow rate of 1 ml/min, the retention time of 6HNic was 7.1 min. The chromatograms were analyzed at 230 and 295 nm using Waters Empower® software. 6HNic concentrations in each sample were determined based on a peak area calibration curve generated using pure 6HNic.

Regulating 6-hydroxy-nicotine

6HNic (InterBioScreen, Moscow, Russia) was prepared as a stock solution of 100 mg/ml in water and used at indicated final concentrations.

RESULTS

Design of the 6-hydroxy-nicotine-responsive mammalian transgene regulation system

Capitalizing on machinery enabling *A.nicotinovorans* pAO1 to metabolize nicotine, we have designed a system called NICE. NICE-controlled transgene modulation in mammalian cells required two functionally crosstalking components: (i) an artificial transactivator (NT1) engineered by fusing *A.nicotinovorans* pAO1's 6-hydroxy-D-nicotine oxidase gene (6HDNO) repressor HdnoR to the generic *H.simplex* type 1 (HSV-1) VP16 transactivation domain (1,38) (pLM82; P_{SV40}-NT1-pA, NT1, HdnoR-VP16) and (ii) a chimeric promoter (P_{NIC}) assembled by cloning 6HDNO-specific operator modules (O_{NIC}) adjacent to a minimal version of the human cytomegalovirus immediate early promoter ($P_{hCMVmin}$; P_{NIC}, O_{NIC}-$P_{hCMVmin}$) (1,39). Following cotransfection of pLM82 (P_{SV40}-NT1-pA) and pLM83 (P_{NIC1a}-SEAP-pA; P_{NIC1a}, O_{NIC}-0bp-$P_{hCMVmin}$), enabling P_{NIC1a}-driven human placental SEAP expression, into CHO-K1 grown in the absence of 6HNic, NT1 bound P_{NIC1a} via HdnoR-O_{NIC} interaction and initiated high-level SEAP production (48.0 ± 7.3 U/l). Akin to 6HNic-mediated derepression of 6HDNO in *A.nicotinovorans* pAO1 NT1 adopts a binding-incompetent allosteric conformation in the presence of 6HNic, which results in disruption of the NT1-P_{NIC1a} interaction and shutdown of SEAP production (1.3 ± 0.2 U/l) (Figure 1).

6HNic-responsive promoter configurations I—P_{NIC} containing a single NT1-specific operator

Efficient transcription-initiation of regulated promoters requires optimal crosstalk between the transcription machinery, the transactivator tethered to the cognate operator and the minimal promoter. The distance and twist between the operator module and the minimal promoter represent spatiosteric constraints for the assembly of the transcription-initiation complex and so influence overall performance of regulated promoters (40–46). With the aim of designing optimal P_{NIC} configurations, we engineered linkers of 2 bp increments ranging from 0 to 10 bp between O_{NIC} and $P_{hCMVmin}$ (P_{NIC1a}, O_{NIC}-0bp-$P_{hCMVmin}$; P_{NIC1b}, O_{NIC}-2bp-$P_{hCMVmin}$; P_{NIC1c}, O_{NIC}-4bp-$P_{hCMVmin}$; P_{NIC1d}, O_{NIC}-6bp-$P_{hCMVmin}$; P_{NIC1e}, O_{NIC}-8bp-$P_{hCMVmin}$; P_{NIC1f}, O_{NIC}-10bp-$P_{hCMVmin}$). $P_{NIC1a-f}$-driven SEAP expression units (P_{NIC1a}, pLM83; P_{NIC1b}, pLM104; P_{NIC1c}, pLM105; P_{NIC1d}, pLM106; P_{NIC1e}, pLM107; P_{NIC1f}, pLM108) were cotransfected with the NT1 expression vector pLM82 (P_{SV40}-NT1-pA) into CHO-K1 and cultivated for 48 h in the presence (50 µg/ml 6HNic) and absence of 6HNic before SEAP production was quantified. The P_{SV40}-driven SEAP expression used as the control indicated that 6HNic showed no negative impact on host cell physiology at regulation-effective concentrations (Figure 2A). P_{NIC1b} harboring 2 bp between O_{NIC} and $P_{hCMVmin}$ showed the tightest repression of all promoter configurations while its maximum SEAP expression levels compared favorably with P_{SV40}. Although P_{NIC1e} and P_{NIC1f} promoted higher SEAP production compared with P_{NIC1b}, their leaky expression was increased as well. Direct comparison of the isogenic promoters P_{NIC1a} and P_{NIC1f}, which harbor O_{NIC} and $P_{hCMVmin}$ on the same face of the DNA but at different distances, suggested a distance-dependent increase of both maximum as well as leaky expression (Figure 2A).

In order to assess the dose-response characteristics of the NICE technology, CHO-K1 were cotransfected with pLM104 (P_{NIC1b}-SEAP-pA) and pLM82 (P_{SV40}-NT1-pA) and cultivated for 48 h in the presence of increasing 6HNic concentrations prior to SEAP production profiling. SEAP production gradually decreased at and beyond 50 ng/ml 6HNic until transgene expression was fully repressed at 50 µg/ml 6HNic. Control configurations including P_{SV40}-driven SEAP expression

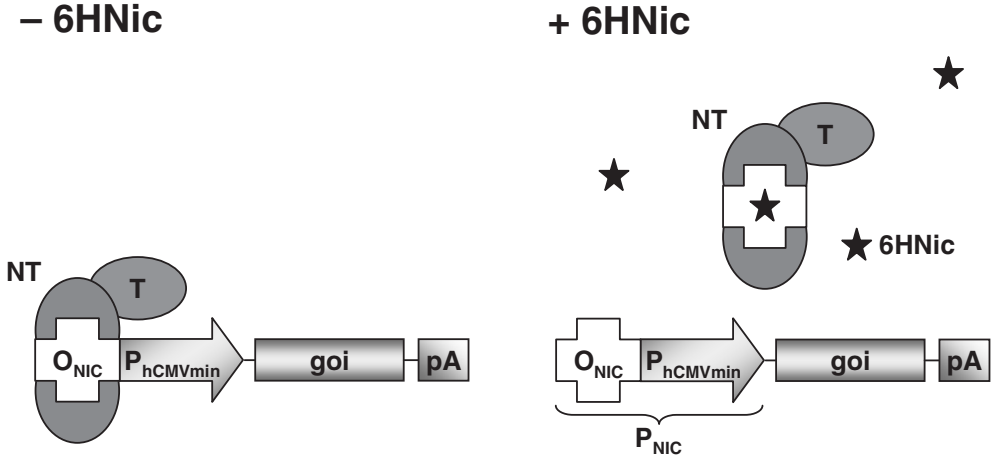

Figure 1. Schematic representation of key components of the 6HNic (6HNic)-responsive transgene regulation system (NICE). As a binary transcription-control system, NICE consists of an artificial 6HNic-dependent transactivator (NT), assembled by fusing the *A.nicotinovorans* pAO1 6HNic oxidase repressor HdnoR to functional mammalian transactivation domains (T; e.g. *H.simplex* VP16, p65 of human NF-κB, a domain of human E2F4) and a chimeric promoter engineered by placing HdnoR-specific operator modules (O_{NIC}) adjacent to a minimal version of the human cytomegalovirus immediate early promoter ($P_{hCMVmin}$). In the absence of 6HNic (−6HNic), NT binds to P_{NIC} via direct HdnoR-O_{NIC} interaction and induces $P_{hCMVmin}$-mediated transcription of the gene of interest (*goi*). However, 6HNic modifies NT's allostery such that it is no longer able to bind and induce P_{NIC}, which results in complete transgene repression.

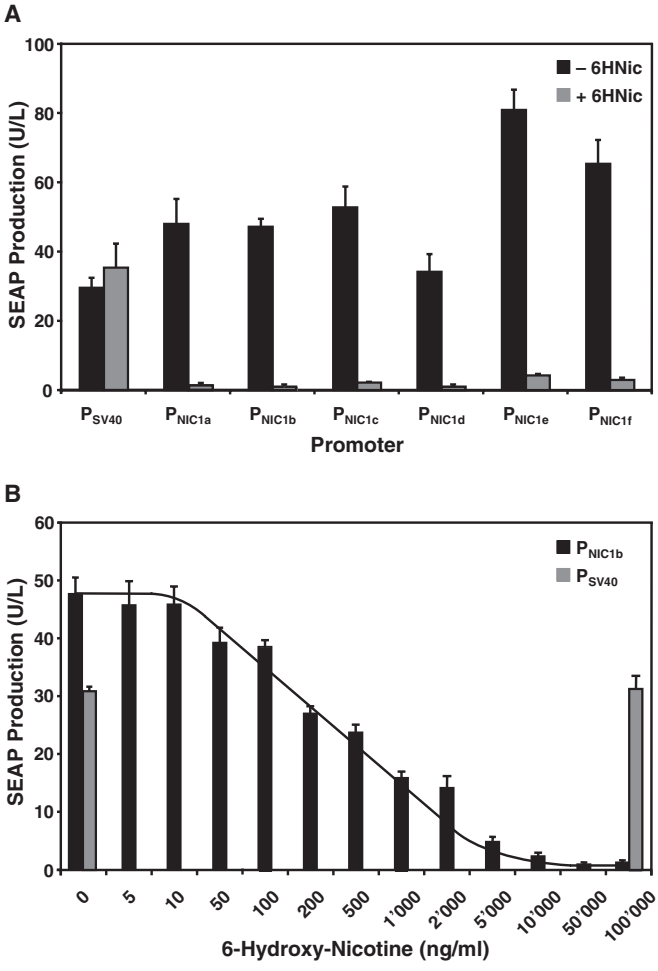

Figure 2. Regulation performance and adjustability of 6HNic-responsive promoters (P_{NIC1}) containing a single 6HNic-dependent transactivator (NT)-specific operator module. (**A**) 6HNic-responsive promoters containing a single operator module (O_{NIC}) were engineered to contain linkers of 2 bp increments ranging from 0 to 10 bp between O_{NIC} and the minimal promoter $P_{hCMVmin}$ (P_{NIC1a}, O_{NIC}-0bp-$P_{hCMVmin}$; P_{NIC1b}, O_{NIC}-2bp-$P_{hCMVmin}$; P_{NIC1c}, O_{NIC}-4bp-$P_{hCMVmin}$; P_{NIC1d}, O_{NIC}-6bp-$P_{hCMVmin}$; P_{NIC1e}, O_{NIC}-8bp-$P_{hCMVmin}$; P_{NIC1f}, O_{NIC}-10bp-$P_{hCMVmin}$). $P_{NIC1a-f}$-driven SEAP expression units (P_{NIC1a}-SEAP-pA [pLM83]; P_{NIC1b}-SEAP-pA [pLM104]; P_{NIC1c}-SEAP-pA [pLM105]; P_{NIC1d}-SEAP-pA [pLM106]; P_{NIC1e}-SEAP-pA [pLM107]; P_{NIC1f}-SEAP-pA [pLM108]) were cotransfected with the NT1 expression vector pLM82 (P_{SV40}-NT1-pA; NT1, HdnoR-VP16) into CHO-K1 and cultivated for 48 h in the presence (50 μg/ml 6HNic) and absence of 6HNic before SEAP production was quantified. SEAP production was compared with pSEAP2-Control-transfected CHO-K1 cells harboring a glycoprotein expression unit driven by the SV40 promoter (P_{SV40}). (**B**) CHO-K1 transfected with pLM82 (P_{SV40}-NT1-pA) and pLM104 (P_{NIC1b}-SEAP-pA) were cultivated for 48 h in the presence of increasing 6HNic concentrations, which resulted in adjustable repression of the model product protein SEAP. (The line was added for clarity.)

in CHO-K1 reached identical glycoprotein production in the absence and presence of 100 μg/ml 6HNic confirming that this nicotine derivative exhibits no deleterious physiologic effects on mammalian cells at regulation-effective concentrations (Figure 2B).

6HNic-responsive promoter configurations II—P_{NIC} containing a tandem NT1-specific operator

In order to increase the expression performance of P_{NIC1b}, we cloned a second O_{NIC} (O_{NIC2}) module 5′ of O_{NIC1}. P_{NIC2} derivatives contain a first NT1 operator (O_{NIC1}) at an optimal distance 5′ of $P_{hCMVmin}$ and a second operator (O_{NIC2}) placed 0/2/4/6/8/10 bp upstream of O_{NIC1} (P_{NIC2}, O_{NIC2}-spacer-O_{NIC1}-NheI-SbfI-4bp-$P_{hCMVmin}$). Resulting promoters (P_{NIC2a}, O_{NIC2}-0bp-O_{NIC1}-NheI-SbfI-4bp-$P_{hCMVmin}$; P_{NIC2b}, O_{NIC2}-2bp-O_{NIC1}-NheI-SbfI-4bp-$P_{hCMVmin}$; P_{NIC2c}, O_{NIC2}-4bp-O_{NIC1}-NheI-SbfI-4bp-$P_{hCMVmin}$; P_{NIC2d}, O_{NIC2}-6bp-O_{NIC1}-NheI-SbfI-4bp-$P_{hCMVmin}$; P_{NIC2e}, O_{NIC2}-8bp-O_{NIC1}-NheI-SbfI-4bp-$P_{hCMVmin}$; P_{NIC2f}, O_{NIC2}-10bp-O_{NIC1}-NheI-SbfI-4bp-$P_{hCMVmin}$) were configured for SEAP expression (pLM135, P_{NIC2a}-SEAP-pA; pLM136, P_{NIC2b}-SEAP-pA; pLM137, P_{NIC2c}-SEAP-pA; pLM138, P_{NIC2d}-SEAP-pA; pLM139, P_{NIC2e}-SEAP-pA; pLM140, P_{NIC2f}-SEAP-pA) and cotransfected with the NT1 expression vector pLM82 (P_{SV40}-NT1-pA) into CHO-K1. Transfected cell populations were grown for 48 h in the presence (50 μg/ml) and absence of 6HNic prior to SEAP quantification (Figure 3). Tandem O_{NIC}-containing modules doubled maximum SEAP expression levels compared with mono-O_{NIC} P_{NIC1} promoter derivatives. However, leaky transcription in the presence of 6HNic was also increased, which compromised overall regulation performance. P_{NIC2d}, containing 6 bp between the two O_{NIC} modules supported optimal tightness among 2-O_{NIC}-containing promoters while transgene expression reached 2-fold higher levels compared with P_{NIC1b} (Figures 2 and 3). Direct correlation between the number of tandem operator modules and maximum expression levels is a common observation for transcription control modalities of the NICE type. Also, a qualitative correlation between maximum and leaky expression is

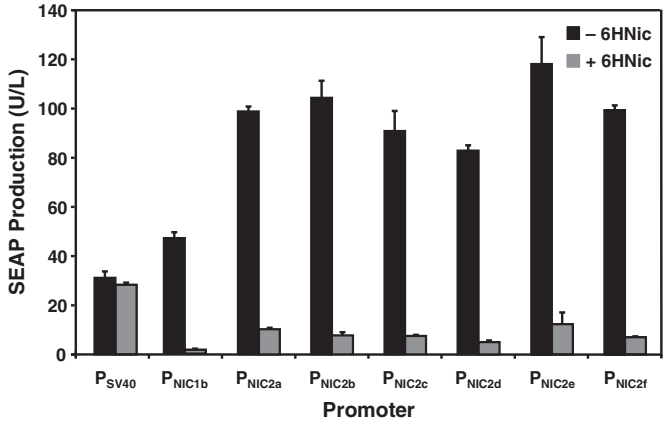

Figure 3. Regulation performance of 6HNic-responsive promoters (P_{NIC2}) containing a twin 6HNic-dependent transactivator (NT)-specific operator module (O_{NIC1} and O_{NIC2}). Whereas the distance of the most proximal O_{NIC1} to the minimal version of the human cytomegalovirus promoter ($P_{hCMVmin}$) was kept constant, the spacing between O_{NIC2} and O_{NIC1} was increased by 2 bp increments (P_{NIC2a}, O_{NIC2}-0bp-O_{NIC1}-NheI-SbfI-4bp-$P_{hCMVmin}$; P_{NIC2b}, O_{NIC2}-2bp-O_{NIC1}-NheI-SbfI-4bp-$P_{hCMVmin}$; P_{NIC2c}, O_{NIC2}-4bp-O_{NIC1}-NheI-SbfI-4bp-$P_{hCMVmin}$; P_{NIC2d}, O_{NIC2}-6bp-O_{NIC1}-NheI-SbfI-4bp-$P_{hCMVmin}$; P_{NIC2e}, O_{NIC2}-8bp-O_{NIC1}-NheI-SbfI-4bp-$P_{hCMVmin}$; P_{NIC2f}, O_{NIC2}-10bp-O_{NIC1}-NheI-SbfI-4bp-$P_{hCMVmin}$). $P_{NIC2a-f}$-driven SEAP expression units (P_{NIC2a}-SEAP-pA [pLM135]; P_{NIC2b}-SEAP-pA [pLM136]; P_{NIC2c}-SEAP-pA [pLM137]; P_{NIC2d}-SEAP-pA [pLM138]; P_{NIC2e}-SEAP-pA [pLM139]; P_{NIC2f}-SEAP-pA [pLM140]) were cotransfected with the NT1 expression vector pLM82 (P_{SV40}-NT1-pA; NT1, HdnoR-VP16) into CHO-K1 and cultivated for 48 h in the presence (50 μg/ml 6HNic) and absence of 6HNic before SEAP production was quantified. SEAP production was compared with pSEAP2-Control-transfected CHO-K1 cells harboring a glycoprotein expression unit driven by the constitutive SV40 promoter (P_{SV40}).

frequently observed (47). Generic P_{NIC1} and P_{NIC2} promoters offer a wide portfolio of transgene regulation performance and provide a choice of specific expression/regulation characteristics, depending on the gene regulation system's mission.

Engineering of different 6HNic-dependent transactivators

In addition to rigorous engineering of 6HNic-responsive promoters, we designed 6HNic-dependent transactivators containing alternative transactivation domains. We selected the potent transactivation domains of NF-κB (p65) and E2F4 (E2F4), which showed efficient transactivation in antibiotic-adjustable transgene regulation settings (47–51). VP16 of NT1 was replaced by p65 and E2F4 transactivation domains, which resulted in NT2 (HdnoR-p65) and NT3 (HdnoR-E2F4), respectively. The relative transactivation properties of NT1, NT2 and NT3 were assessed by cotransfection of either pLM82 (P_{SV40}-NT1-pA), pLM101 (P_{SV40}-NT2-pA) or pLM102 (P_{SV40}-NT3-pA) and pLM104 (P_{NIC1b}-SEAP-pA) into CHO-K1 followed by cultivation for 48 h in the presence and absence of 6HNic and SEAP quantification (Figure 4). Although all transactivators mediated comparable basal expression levels, their maximum transgene production levels differed significantly. NT2's transactivation efficiency was lower compared with NT1 but higher than NT3. Thus, 6HNic-dependent transactivators showed graded transcription-initiation capacity and provided a choice of different expression windows.

Development of 6HNic-adjustable lentivectors

In order to enable straightforward one-step engineering of mammalian cells for NICE-controlled transgene expression, we have designed a set of HIV-1-derived self-inactivating lentiviral expression vectors exemplified by pLM141 (5′LTR-ψ$^+$-ori$_{SV40}$-PPT-RRE-P_{NIC2d}-SEAP-3′$LTR_{\Delta U3}$) and pLM103 (5′LTR-ψ$^+$-ori$_{SV40}$-PPT-RRE-$P_{hEF1\alpha}$-NT1-3′$LTR_{\Delta U3}$). Cotransduction of pLM141- and pLM103-derived lentiviral particles into CHO-K1 followed by cultivation of engineered cell populations at increasing 6HNic concentrations resulted in precise dose-dependent SEAP expression fine-tuning (Figure 5A). Besides excellent adjustability, NICE-controlled SEAP production was fully reversible when followed over a 1 week period of 6HNic addition and removal alternating every 48 h. SEAP accumulation kinetics, maximum expression levels in the absence and basal expression levels in the presence of 50 μg/ml 6HNic remained reproducible following consecutive expression status switches (Figure 5B). Repeated ON–OFF or OFF–ON expression switching did neither compromise maximum nor basal expression levels.

In parallel, we studied the impact of repressed or induced expression status imprinting on follow-up expression scenarios. CHO-K1 transduced for NICE-controlled SEAP expression were set for 48 h to high (0, −6HNic) or basal (1, +6HNic) glycoprotein production, which was either maintained or switched twice during subsequent 48 h cultivation periods (48 h → 48 h → 48 h; 0 → 0 → 0, 0 → 0 → 1, 0 → 1 → 0, 0 → 1 → 1, 1 → 0 → 0, 1 → 0 → 1, 1 → 1 → 0, 1 → 1 → 1). Irrespective of the cell population's previous NICE-controlled expression history, SEAP production levels in the presence or absence of 6HNic remained consistent (Figure 5C). Lentiviral implementation of NICE-controlled fine-tuning of transgene expression enabled stable, adjustable and reversible regulation characteristics as well as sustained regulation kinetics for over 6 days.

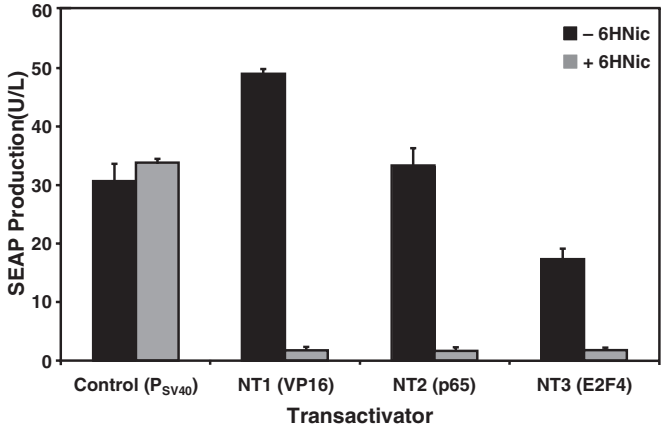

Figure 4. Regulation performance of different 6HNic-dependent transactivators. *A.nicotinovorans* pAO1's 6HNic oxidase repressor HdnoR was fused to different transactivation domains derived from (i) *H.simplex* virus (VP16; NT1, HdnoR-VP16), (ii) human NF-κB (p65; NT2, HdnoR-p65) and (iii) human E2F4 (E2F4; NT3, HdnoR-E2F4). The regulation performance of NT1, NT2 and NT3 was assessed by cotransfection of either pLM82 (P_{SV40}-NT1-pA), pLM101 (P_{SV40}-NT2-pA) or pLM102 (P_{SV40}-NT3-pA) and pLM104 (P_{NIC1b}-SEAP-pA) into CHO-K1 followed by cultivation for 48 h in the presence and absence of 6HNic and SEAP quantification. SEAP production was compared with pSEAP2-Control-transfected CHO-K1 cells harboring a glycoprotein expression unit driven by the constitutive SV40 promoter (P_{SV40}).

In vivo validation of NICE-adjustable transgene expression in mice and chicken embryos

For *in vivo* validation of NICE-adjustable transgene expression, we implanted microencapsulated CHO-K1 cells transgenic for NICE-controlled SEAP expression into coherent alginate-poly-L-lysine-alginate capsules intraperitoneally into mice (200 cells/capsule). Treated mice were exposed to different daily 6HNic doses, and serum SEAP levels were quantified 72 h after implantation. While NICE-induced SEAP production resulted in high-level concentrations of this glycoprotein in the serum of treated mice (106 ± 21 mU/l), 6HNic was unable to repress heterologous production even at concentrations of 100 mg/kg. 6HNic is a unique unphysiologic compound, which may fail to control NICE-driven gene expression due to unknown *in vivo* derivatization/degradation or rapid clearance from the body. Indeed, HPLC-based analysis of urine samples collected from 6HNic-treated mice showed that 90% of the administered nicotine derivative was excreted after 2 h (Figure 6). Therefore, further efforts will be required to establish NICE technology in mammals. However, the 6HNic concentration administered to mice without significant side effects remains impressive and holds promises for future applications.

In order to alleviate possible 6HNic clearance, we cotransduced chicken embryos with lentiviral particles derived from pLM103- (5′LTR-ψ$^+$-ori$_{SV40}$-cPPT-RRE-$P_{hEF1\alpha}$-NT1-3′$LTR_{\Delta U3}$) and pLM146- (5′LTR-ψ$^+$-ori$_{SV40}$-cPPT-RRE-P_{NIC3}-$VEGF_{121}$-3′$LTR_{\Delta U3}$). The pLM146 lentivector harbors a P_{NIC3} (O_{NIC}-4bp-NheI-SbfI-$P_{hCMVmin}$)-driven human

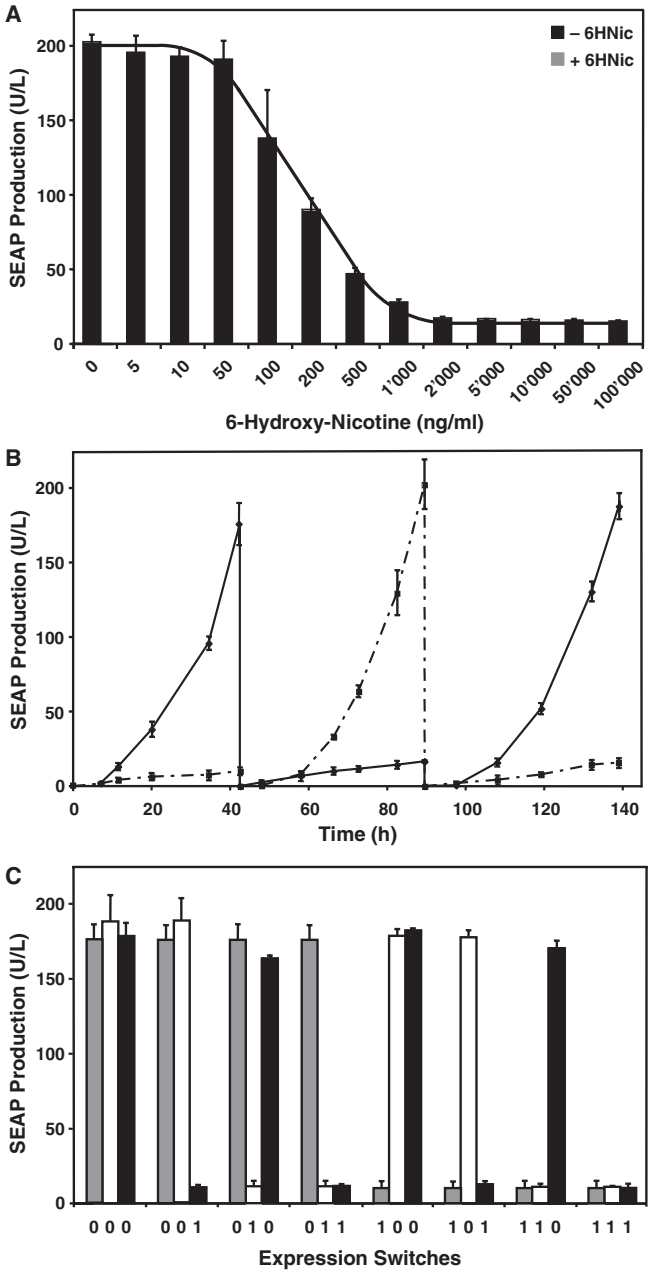

Figure 5. Adjustability, reversibility and expression imprinting of NICE-controlled transgene transduction using HIV-1-derived lentiviral particles. (**A**) 6HNic-adjustable SEAP expression of CHO-K1 cells cotransduced with pLM103- (5′LTR-ψ^+-ori$_{SV40}$-cPPT-RRE-P$_{hEF1\alpha}$-NT1-3′LTR$_{\Delta U3}$) and pLM141- (5′LTR-ψ^+-ori$_{SV40}$-cPPT-RRE-P$_{NIC2d}$-SEAP-3′LTR$_{\Delta U3}$) derived lentiviral particles. Transduced cells were grown for 48 h in medium supplemented with increasing 6HNic concentrations prior to SEAP production profiling (The line was added for clarity). (**B**) Reversibility of NICE-controlled transgene transduction. Aforementioned CHO-K1 cell populations (40 000 cells/ml) transduced with pLM103/141-derived lentiviral particles were cultivated in the presence and absence of 6HNic (50 μg/ml). The SEAP expression status (presence of 6HNic, OFF; absence of 6HNic, ON) was reversed and quantified on alternate days (48, 96 and 144 h) after culture medium exchanges. (**C**) Assessment of expression imprinting of NICE-controlled transgene transduction. CHO-K1 transduced for NICE-controlled SEAP expression were set for 48 h to high (0, −6HNic) or basal (1, +6HNic) glycoprotein production, which was then either maintained or switched twice during subsequent 48 h cultivation periods (48 h → 48 h → 48 h; 0 → 0 → 0, 0 → 0 → 1, 0 → 1 → 0, 0 → 1 → 1, 1 → 0 → 0, 1 → 0 → 1, 1 → 1 → 0, 1 → 1 → 1).

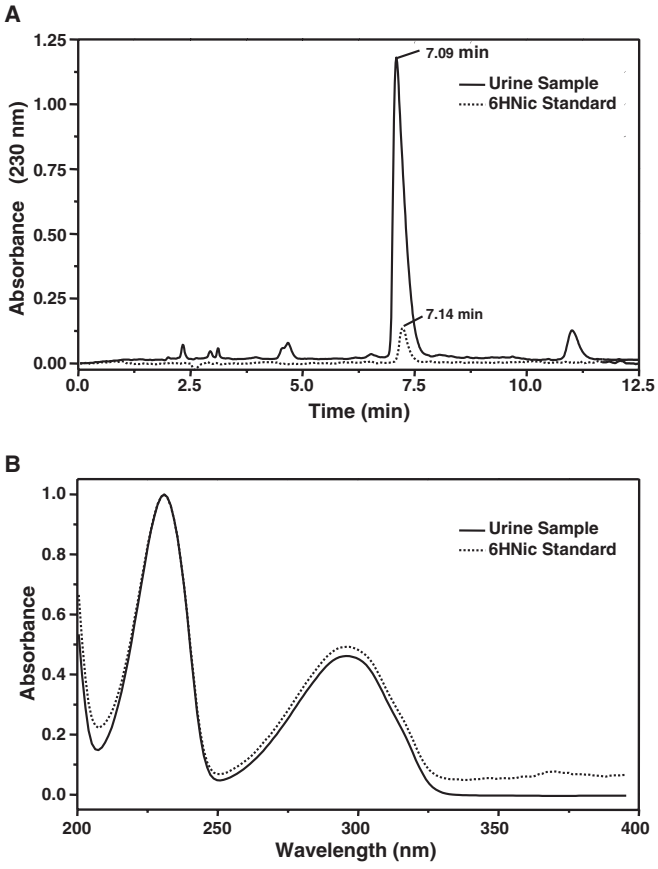

Figure 6. HPLC-based 6HNic analysis of mouse urine samples. (**A**) Chromatograms of a 6HNic standard (2.5 nmol, 0.45 μg; dotted line) and a urine sample collected from mice 2 h after intraperitoneal injection of 20 mg/kg 6HNic (solid line). (**B**) Comparative UV spectra of the peaks at 7.09 and 7.14 min [see (A)].

$VEGF_{121}$ expression cassette to modulate the chicken embryo's vascularization in a 6HNic-adjustable manner (Figure 7). Cotransduction of these lentiviral particles into CHO-K1 followed by cultivation of infected cell populations at increasing 6HNic concentrations resulted in tight dose-dependent $VEGF_{121}$ expression fine-tuning (Figure 8). Microscopic analysis of $VEGF_{121}$-mediated neovascularization, as well as vessel morphology in the CAM of chicken embryos grown for 3 days at decreasing 6HNic concentrations or 6HNic-free conditions (50, 1, 0.1, 0 μg/ml, see Figure 7) showed a dose-dependent angiogenic response characterized by a general increase in blood vessel number, atypical (brush- and delta-like) endpoint patterns, irregular tortuous vessel shape and multiple vessel branching. All of those effects could be completely repressed by treating the chicken embryo with 50 μg/ml 6HNic. $VEGF_{121}$-induced impact on vessel structure was confined to a 4 mm radius around the site of lentiviral particle application and could not be observed on the same CAM beyond this perimeter (Figure 7). These results confirm 6HNic-adjustable transgene transduction *in vivo*.

DISCUSSION

Long appreciated in basic sciences for their power to reveal gene-function correlations, heterologous transgene control systems have gathered momentum and now stand on the eve

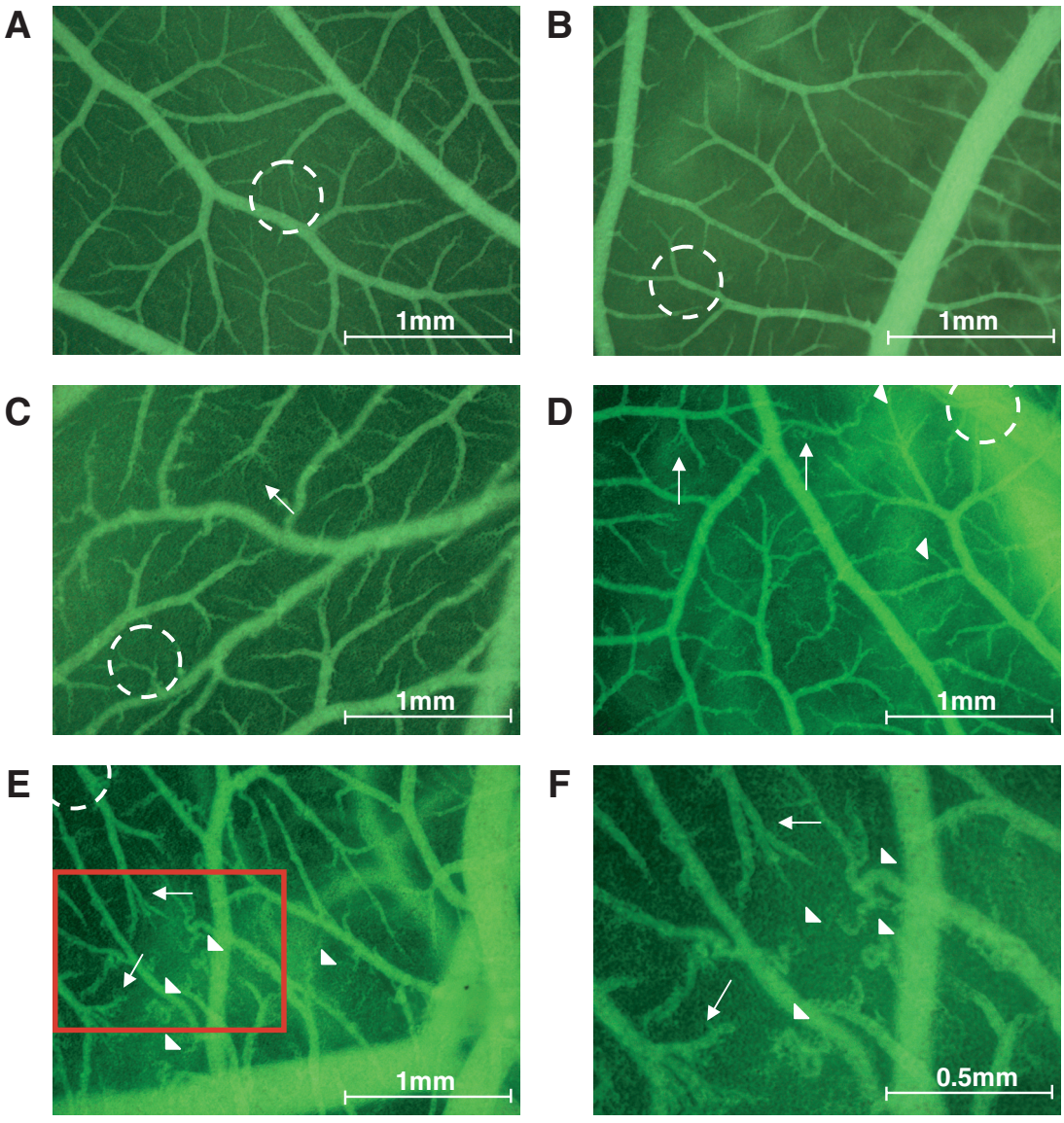

Figure 7. *In vivo* microscopy of angiogenic response in the CAM of 12-day-old chicken embryos 72 h post cotransduction with lentiviral particles derived from pLM103- (5′LTR-ψ^+-ori$_{SV40}$-cPPT-RRE-P$_{hEF1\alpha}$-NT1-3′LTR$_{\Delta U3}$) and pLM146- (5′LTR-ψ^+-ori$_{SV40}$-cPPT-RRE-P$_{NIC3}$-VEGF$_{121}$-3′LTR$_{\Delta U3}$). Following administration of 50 μg/ml 6HNic 1 h post transduction, NICE-controlled VEGF$_{121}$ production was completely repressed (**A**) and microvascular growth compared with mock-transduced 6HNic-treated control embryos (**B**). Transduced cultures treated with decreasing 6HNic concentrations showed an increasing dose-dependent angiogenic response with atypical (brush- and delta-like) endpoint patterns (arrows) and irregular tortuous vessel shape (arrowhead) within a perimeter of 4 mm of the transduction site (dashed circle). [(**C**) 1 μg/ml 6HNic; (**D**) 0.1 μg/ml 6HNic; (**E**) no 6HNic; see Figure 8 for VEGF$_{121}$ expression profiles.] (**F**) Detail representation of the red-framed part of D.

of therapeutic and pilot production implementation (20,52). Currently available transcription control modalities capitalize on the generic design principle of the pioneering TET system: (i) clinically licensed tetracycline as inducer, (ii) bacterial repressor fused to mammalian cell-compatible transactivation domain as transactivator and (iii) transactivator-specific promoter assembled by fusing transactivator-specific operator modules to a minimal eukaryotic promoter. Besides their relationship to the TET configuration alternative transgene control systems differ significantly in the regulating small molecule (clinically licensed small-molecule drugs [antibiotics (7,9–11), immunosuppressive agents, (12), hormones and hormone agonists, (13–15), type-2 diabetes drug, (19,53), clinically inert compounds (17,18), temperature (16) and gaseous acetaldehyde (20)]), the origin of the transactivator [prokaryotic origin (7,9–11,16–18,20) (http://www.qbiogene.com/products/gene-expression/qmateslideshow/index.htm), mammalian origin (13,14,19,53)] and their promoter configurations [tandem operator modules, minimal promoter origin, relative promoter-operator spacing; see (40) as well as (52) for a non-limiting overview]. Despite the portfolio of different transgene regulation systems, there is nothing like the best control modality. All systems are associated with pros and cons:

(i) clinically licensed inducers are intuitively better suited for therapeutic applications, although ongoing administration of small-molecule drugs is prone to side effects,

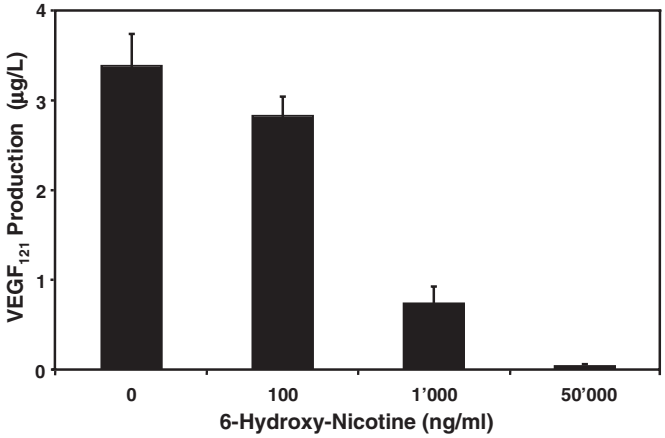

Figure 8. Dose–response characteristics of P_{NIC3}-driven $VEGF_{121}$ expression engineered into a lentiviral expression configuration. CHO-K1 cells were cotransduced with pLM103 lentiviral particles derived from (5′LTR-ψ$^+$-ori$_{SV40}$-cPPT-RRE-P$_{hEF1\alpha}$-NT1-3′LTR$_{\Delta U3}$)- and pLM146 (5′LTR-ψ$^+$-ori$_{SV40}$-cPPT-RRE-P_{NIC3}-$VEGF_{121}$-3′LTR$_{\Delta U3}$) and grown for 48 h in medium supplemented with increasing 6HNic concentrations before $VEGF_{121}$ production was quantified.

(ii) prokaryotic-derived promoter-transactivator systems operate in the absence of pleiotropies, yet may elicit immune responses,
(iii) eukaryotic-derived promoter-transactivator systems are compatible with the immune system, yet may interfere with endogenous regulatory networks.

The demands for transgene control modalities are as different as the systems themselves: while the gene therapy and tissue engineering communities prefer endogenous regulation systems adjusted by clinically licensed small-molecule drugs, biopharmaceutical manufacturing representatives favor heterologous prokaryotic-derived systems fine-tuned by clinically inert compounds.

Based on the components of *A.nicotinovorans* pAO1's nicotine mobilization machinery, we have designed a novel gene control system to adjust transgene expression in response to the water-soluble nicotine derivative 6HNic. The NICE technology mediated high-level expression, tight repression, precise expression fine-tuning and reversible transcription control in the absence of compromising imprinting originating from previous switching history. All of those performance characteristics have been confirmed in a variety of expression configurations in mammalian cells, by lentivirus-mediated transduction as well as in chicken embryos. As a closed system, chicken embryos supported adjustable angiogenic responses *in vivo*. However, 6HNic was unable to modulate SEAP expression in mice, suggesting that its high water solubility promoted rapid renal clearance and resulted in control-incompatible pharmacokinetics in whole animals.

Starting with a generic design concept, we have improved the NICE technology by (i) varying O_{NIC}-$P_{hCMVmin}$ spacing, (ii) engineering tandem O_{NIC} repeats and modifying the inter-O_{NIC} distance and by (iii) swapping the transactivation domains fused to HdnoR. In order to selectively improve the regulation performance of hybrid NICE promoters, we focused on optimizing the spatio-steric relation between promoter, transactivator and transcription-initiation complex. The importance of rotational alignment of *cis*-acting elements on overall promoter performance has been investigated in several systems. The synthesis of those studies suggested appropriate helical phasing to be required for optimal promoter activity. Non-limiting examples included the promoter of the human serine protease B gene (54), the promoter of the *Escherichia coli araBAD* operon (55) and the promoter of the human HLA-DR gene (56). Furthermore, helical periodicity has been observed for promoter-enhancer crosstalk in SV40 and HIV-1 viruses (57,58). As for heterologous gene regulation systems, Weber and co-workers (47) have recently exemplified that the spacing and torsion angle between the operator and minimal promoters had dramatic impact on the overall regulation performance. This observation could be confirmed for the NICE system. Increasing the O_{NIC}-$P_{hCMVmin}$ distance by 2 bp increments resulted in a promoter portfolio with graded response characteristics.

It is commonly accepted that transactivator-mediated transcription-initiation increases with the number of cognate operator modules (59,60). Similarly, NICE promoters harboring tandem operator modules showed 2- to 3-fold higher transgene expression compared with mono O_{NIC}-containing promoters. The net increase of the maximum expression levels was a function of the inter-O_{NIC} distance. The relative spacing between different operator modules has long been recognized as an essential factor for promoter performance (46,61–65). For example, analysis of beta interferon (IFN-β) gene activation showed that deletion,or rearrangement of any one of the enhancer modules compromises transcription performance (66). Also, variation of the spacing between individual activator binding sites within the TCR α enhancer modulated enhancer activity in a helical phasing-dependent manner (67). We have modified the inter-O_{NIC} spacing by 2 bp increments while leaving the tandem operator-minimal promoter distance invariant. Optimal spacing resulted in up to 3-fold increased maximum expression levels. However, basal expression was higher as well.

Since the transactivator interfaces with promoter and transcription-initiation machinery it has a decisive impact on the overall regulation and expression performance of transgene control modalities. We have therefore equipped HdnoR with different viral and human transactivation domains, which mediated graded response characteristics in CHO-K1.

The NICE optimization studies have resulted in a portfolio of different 6HNic-responsive promoter/transactivator configurations, which show superior key characteristics including tight repression and maximum expression levels. The choice of different promoter/transactivator combinations enables unmatched adaptation of NICE-controlled transgene expression to specific needs: tight repression is best satisfied by mono-O_{NIC}-containing promoters while promoters with tandem O_{NIC} modules support high-level transgene expression. Our rigorous NICE analysis has exemplified its potential for sophisticated cell engineering related to basic and applied research applications.

ACKNOWLEDGEMENTS

The authors thank Roderich Brandsch for providing pH6EX3-HdnoR. This work was supported by the Swiss National Science Foundation (grant no. 631-065946) as well as the

Swiss State Secretariat for Education and Research within EC Framework 6. Funding to pay the Open Access publication charges for this article was provided by ETH Zurich.

Conflict of interest statement. None declared.

REFERENCES

1. Sandu,C., Chiribau,C.B. and Brandsch,R. (2003) Characterization of HdnoR, the transcriptional repressor of the 6-hydroxy-D-nicotine oxidase gene of *Arthrobacter nicotinovorans* pAO1, and its DNA-binding activity in response to L- and D-nicotine derivatives. *J. Biol. Chem.*, **278**, 51307–51315.
2. Schmid,A., Dordick,J.S., Hauer,B., Kiener,A., Wubbolts,M. and Witholt,B. (2001) Industrial biocatalysis today and tomorrow. *Nature*, **409**, 258–268.
3. Brenik,W. and Rudhard,H. (1982) Patent US4343318.
4. Gravely,L.E., Geiss,V.L. and Gregory,C.F. (1985) United States Patent US4557280.
5. Yildiz,D. (2004) Nicotine, its metabolism and an overview of its biological effects. *Toxicon*, **43**, 619–632.
6. Hillen,W., Klock,G., Kaffenberger,I., Wray,L.V. and Reznikoff,W.S. (1982) Purification of the TET repressor and TET operator from the transposon Tn10 and characterization of their interaction. *J. Biol. Chem.*, **257**, 6605–6613.
7. Gossen,M. and Bujard,H. (1992) Tight control of gene expression in mammalian cells by tetracycline-responsive promoters. *Proc. Natl Acad. Sci. USA*, **89**, 5547–5551.
8. Gossen,M., Freundlieb,S., Bender,G., Muller,G., Hillen,W. and Bujard,H. (1995) Transcriptional activation by tetracyclines in mammalian cells. *Science*, **268**, 1766–1769.
9. Fussenegger,M., Morris,R.P., Fux,C., Rimann,M., von Stockar,B., Thompson,C.J. and Bailey,J.E. (2000) Streptogramin-based gene regulation systems for mammalian cells. *Nat. Biotechnol.*, **18**, 1203–1208.
10. Weber,W., Fux,C., Daoud-el Baba,M., Keller,B., Weber,C.C., Kramer,B.P., Heinzen,C., Aubel,D., Bailey,J.E. and Fussenegger,M. (2002) Macrolide-based transgene control in mammalian cells and mice. *Nat. Biotechnol.*, **20**, 901–907.
11. Zhao,H.F., Boyd,J., Jolicoeur,N. and Shen,S.H. (2003) A coumermycin/novobiocin-regulated gene expression system. *Hum. Gene Ther.*, **14**, 1619–1629.
12. Rivera,V.M., Clackson,T., Natesan,S., Pollock,R., Amara,J.F., Keenan,T., Magari,S.R., Phillips,T., Courage,N.L., Cerasoli,F.Jr *et al.* (1996) A humanized system for pharmacologic control of gene expression. *Nature Med.*, **2**, 1028–1032.
13. Braselmann,S., Graninger,P. and Busslinger,M. (1993) A selective transcriptional induction system for mammalian cells based on Gal4-estrogen receptor fusion proteins. *Proc. Natl Acad. Sci. USA*, **90**, 1657–1661.
14. Beerli,R.R., Schopfer,U., Dreier,B. and Barbas,C.F.,III (2000) Chemically regulated zinc finger transcription factors. *J. Biol. Chem.*, **275**, 32617–32627.
15. No,D., Yao,T.P. and Evans,R.M. (1996) Ecdysone-inducible gene expression in mammalian cells and transgenic mice. *Proc. Natl Acad. Sci. USA*, **93**, 3346–3351.
16. Weber,W., Marty,R.R., Link,N., Ehrbar,M., Keller,B., Weber,C.C., Zisch,A.H., Heinzen,C., Djonov,V. and Fussenegger,M. (2003) Conditional human VEGF-mediated vascularization in chicken embryos using a novel temperature-inducible gene regulation (TIGR) system. *Nucleic Acids Res.*, **31**, e69.
17. Weber,W., Schoenmakers,R., Spielmann,M., El-Baba,M.D., Folcher,M., Keller,B., Weber,C.C., Link,N., van de Wetering,P., Heinzen,C. *et al.* (2003) *Streptomyces*-derived quorum-sensing systems engineered for adjustable transgene expression in mammalian cells and mice. *Nucleic Acids Res.*, **31**, e71.
18. Weber,W., Malphettes,L., de Jesus,M., Schoenmakers,R., El-Baba,M.D., Spielmann,M., Keller,B., Weber,C.C., van de Wetering,P., Aubel,D. *et al.* (2004) Engineered *Streptomyces* quorum-sensing components enable inducible siRNA-mediated translation control in mammalian cells and adjustable transcription control in mice. *J. Gene Med.*, **7**, 518–525.
19. Tascou,S., Sorensen,T.K., Glenat,V., Wang,M., Lakich,M.M., Darteil,R., Vigne,E. and Thuillier,V. (2004) Stringent rosiglitazone-dependent gene switch in muscle cells without effect on myogenic differentiation. *Mol. Ther.*, **9**, 637–649.
20. Weber,W., Rimann,M., Spielmann,M., Keller,B., Daoud-El Baba,M., Aubel,D., Weber,C.C. and Fussenegger,M. (2004) Gas-inducible transgene expression in mammalian cells and mice. *Nat. Biotechnol.*, **22**, 1440–1444.
21. Beck,C., Uramoto,H., Boren,J. and Akyurek,L.M. (2004) Tissue-specific targeting for cardiovascular gene transfer. Potential vectors and future challenges. *Curr. Gene Ther.*, **4**, 457–467.
22. Aubel,D., Morris,R., Lennon,B., Rimann,M., Kaufmann,H., Folcher,M., Bailey,J.E., Thompson,C.J. and Fussenegger,M. (2001) Design of a novel mammalian screening system for the detection of bioavailable, non-cytotoxic streptogramin antibiotics. *J. Antibiot. (Tokyo)*, **54**, 44–55.
23. Gonzalez-Nicolini,V., Fux,C. and Fussenegger,M. (2004) A novel mammalian cell-based approach for the discovery of anticancer drugs with reduced cytotoxicity on non-dividing cells. *Invest. New Drugs*, **22**, 253–262.
24. Umaña,P., Jean-Mairet,J. and Bailey,J.E. (1999) Tetracycline-regulated overexpression of glycosyltransferases in Chinese hamster ovary cells. *Biotechnol. Bioeng.*, **65**, 542–549.
25. Fussenegger,M., Schlatter,S., Datwyler,D., Mazur,X. and Bailey,J.E. (1998) Controlled proliferation by multigene metabolic engineering enhances the productivity of Chinese hamster ovary cells. *Nat. Biotechnol.*, **16**, 468–472.
26. Malleret,G., Haditsch,U., Genoux,D., Jones,M.W., Bliss,T.V., Vanhoose,A.M., Weitlauf,C., Kandel,E.R., Winder,D.G. and Mansuy,I.M. (2001) Inducible and reversible enhancement of learning, memory, and long-term potentiation by genetic inhibition of calcineurin. *Cell*, **104**, 675–686.
27. Cohlan,S.Q. (1977) Tetracycline staining of teeth. *Teratology*, **15**, 127–129.
28. Lautermann,J., Dehne,N., Schacht,J. and Jahnke,K. (2004) [Aminoglycoside- and cisplatin-ototoxicity: from basic science to clinics.]. *Laryngorhinootologie*, **83**, 317–323.
29. Sartor,O. and Cutler,G.B.,Jr (1996) Mifepristone: treatment of Cushing's syndrome. *Clin. Obstet Gynecol.*, **39**, 506–510.
30. Kramer,B.P., Weber,W. and Fussenegger,M. (2003) Artificial regulatory networks and cascades for discrete multilevel transgene control in mammalian cells. *Biotechnol. Bioeng.*, **83**, 810–820.
31. Kramer,B.P., Viretta,A.U., Daoud-El-Baba,M., Aubel,D., Weber,W. and Fussenegger,M. (2004) An engineered epigenetic transgene switch in mammalian cells. *Nat. Biotechnol.*, **22**, 867–870.
32. Kramer,B.P., Fischer,C. and Fussenegger,M. (2004) BioLogic gates enable logical transcription control in mammalian cells. *Biotechnol. Bioeng.*, **87**, 478–484.
33. Mitta,B., Rimann,M., Ehrengruber,M.U., Ehrbar,M., Djonov,V., Kelm,J. and Fussenegger,M. (2002) Advanced modular self-inactivating lentiviral expression vectors for multigene interventions in mammalian cells and *in vivo* transduction. *Nucleic Acids Res.*, **30**, e113.
34. Reiser,J., Harmison,G., Kluepfel-Stahl,S., Brady,R.O., Karlsson,S. and Schubert,M. (1996) Transduction of nondividing cells using pseudotyped defective high-titer HIV type 1 particles. *Proc. Natl Acad. Sci. USA*, **93**, 15266–15271.
35. Mochizuki,H., Schwartz,J.P., Tanaka,K., Brady,R.O. and Reiser,J. (1998) High-titer human immunodeficiency virus type 1-based vector systems for gene delivery into nondividing cells. *J. Virol.*, **72**, 8873–8883.
36. Djonov,V., Schmid,M., Tschanz,S.A. and Burri,P.H. (2000) Intussusceptive angiogenesis: its role in embryonic vascular network formation. *Circ. Res.*, **86**, 286–292.
37. Djonov,V.G., Galli,A.B. and Burri,P.H. (2000) Intussusceptive arborization contributes to vascular tree formation in the chick chorio-allantoic membrane. *Anat. Embryol. (Berl.)*, **202**, 347–357.
38. Herrera,F.J. and Triezenberg,S.J. (2004) VP16-dependent association of chromatin-modifying coactivators and underrepresentation of histones at immediate-early gene promoters during herpes simplex virus infection. *J. Virol.*, **78**, 9689–9696.
39. Boshart,M., Weber,F., Jahn,G., Dorsch-Hasler,K., Fleckenstein,B. and Schaffner,W. (1985) A very strong enhancer is located upstream of an immediate early gene of human cytomegalovirus. *Cell*, **41**, 521–530.
40. Weber,W. and Fussenegger,M. (2002) Artificial mammalian gene regulation networks-novel approaches for gene therapy and bioengineering. *J. Biotechnol.*, **98**, 161–187.

41. Semsey,S., Geanacopoulos,M., Lewis,D.E. and Adhya,S. (2002) Operator-bound GalR dimers close DNA loops by direct interaction: tetramerization and inducer binding. *EMBO J.*, **21**, 4349–4356.
42. Sathya,G., Li,W., Klinge,C.M., Anolik,J.H., Hilf,R. and Bambara,R.A. (1997) Effects of multiple estrogen responsive elements, their spacing, and location on estrogen response of reporter genes. *Mol. Endocrinol.*, **11**, 1994–2003.
43. Schreiter,E.R., Sintchak,M.D., Guo,Y., Chivers,P.T., Sauer,R.T. and Drennan,C.L. (2003) Crystal structure of the nickel-responsive transcription factor NikR. *Nature Struct. Biol.*, **10**, 794–799.
44. Parkhill,J. and Brown,N.L. (1990) Site-specific insertion and deletion mutants in the mer promoter-operator region of Tn501; the nineteen base-pair spacer is essential for normal induction of the promoter by MerR. *Nucleic Acids Res.*, **18**, 5157–5162.
45. Brown,N.L., Stoyanov,J.V., Kidd,S.P. and Hobman,J.L. (2003) The MerR family of transcriptional regulators. *FEMS Microbiol Rev.*, **27**, 145–163.
46. Lewis,D.E. and Adhya,S. (2002) *In vitro* repression of the gal promoters by GalR and HU depends on the proper helical phasing of the two operators. *J. Biol. Chem.*, **277**, 2498–2504.
47. Weber,W., Kramer,B.P., Fux,C., Keller,B. and Fussenegger,M. (2002) Novel promoter/transactivator configurations for macrolide- and streptogramin-responsive transgene expression in mammalian cells. *J. Gene Med.*, **4**, 676–686.
48. Schmitz,M.L., Stelzer,G., Altmann,H., Meisterernst,M. and Baeuerle,P.A. (1995) Interaction of the COOH-terminal transactivation domain of p65 NF-kappa B with TATA-binding protein, transcription factor IIB, and coactivators. *J. Biol. Chem.*, **270**, 7219–7226.
49. Urlinger,S., Helbl,V., Guthmann,J., Pook,E., Grimm,S. and Hillen,W. (2000) The p65 domain from NF-kappaB is an efficient human activator in the tetracycline-regulatable gene expression system. *Gene*, **247**, 103–110.
50. Akagi,K., Kanai,M., Saya,H., Kozu,T. and Berns,A. (2001) A novel tetracycline-dependent transactivator with E2F4 transcriptional activation domain. *Nucleic Acids Res.*, **29**, E23.
51. Baron,U., Gossen,M. and Bujard,H. (1997) Tetracycline-controlled transcription in eukaryotes: novel transactivators with graded transactivation potential. *Nucleic Acids Res.*, **25**, 2723–2729.
52. Weber,W. and Fussenegger,M. (2004) Inducible gene expression in mammalian cells and mice. *Methods Mol. Biol.*, **267**, 451–466.
53. Wang,Y., O'Malley,B.W.,Jr, Tsai,S.Y. and O'Malley,B.W. (1994) A regulatory system for use in gene transfer. *Proc. Natl Acad. Sci. USA*, **91**, 8180–8184.
54. Hanson,R.D., Grisolano,J.L. and Ley,T.J. (1993) Consensus AP-1 and CRE motifs upstream from the human cytotoxic serine protease B (CSP-B/CGL-1) gene synergize to activate transcription. *Blood*, **82**, 2749–2757.
55. Dunn,T.M., Hahn,S., Ogden,S. and Schleif,R.F. (1984) An operator at -280 base pairs that is required for repression of araBAD operon promoter: addition of DNA helical turns between the operator and promoter cyclically hinders repression. *Proc. Natl Acad. Sci. USA*, **81**, 5017–5020.
56. Vilen,B.J., Cogswell,J.P. and Ting,J.P. (1991) Stereospecific alignment of the X and Y elements is required for major histocompatibility complex class II DRA promoter function. *Mol. Cell Biol.*, **11**, 2406–2415.
57. Takahashi,K., Vigneron,M., Matthes,H., Wildeman,A., Zenke,M. and Chambon,P. (1986) Requirement of stereospecific alignments for initiation from the simian virus 40 early promoter. *Nature*, **319**, 121–126.
58. Rao,E., Dang,W., Tian,G. and Sen,R. (1997) A three-protein-DNA complex on a B cell-specific domain of the immunoglobulin mu heavy chain gene enhancer. *J. Biol. Chem.*, **272**, 6722–6732.
59. Ellwood,K., Huang,W., Johnson,R. and Carey,M. (1999) Multiple layers of cooperativity regulate enhanceosome-responsive RNA polymerase II transcription complex assembly. *Mol. Cell Biol.*, **19**, 2613–2623.
60. Wang,J., Ellwood,K., Lehman,A., Carey,M.F. and She,Z.S. (1999) A mathematical model for synergistic eukaryotic gene activation. *J. Mol. Biol.*, **286**, 315–325.
61. Hebner,C., Lasanen,J., Battle,S. and Aiyar,A. (2003) The spacing between adjacent binding sites in the family of repeats affects the functions of Epstein-Barr nuclear antigen 1 in transcription activation and stable plasmid maintenance. *Virology*, **311**, 263–274.
62. Nikolajczyk,B.S., Nelsen,B. and Sen,R. (1996) Precise alignment of sites required for mu enhancer activation in B cells. *Mol. Cell Biol.*, **16**, 4544–4554.
63. Xiong,G. and Maser,E. (2001) Regulation of the steroid-inducible 3alpha-hydroxysteroid dehydrogenase/carbonyl reductase gene in *Comamonas testosteroni*. *J. Biol. Chem.*, **276**, 9961–9970.
64. Chi,T., Lieberman,P., Ellwood,K. and Carey,M. (1995) A general mechanism for transcriptional synergy by eukaryotic activators. *Nature*, **377**, 254–257.
65. Lederer,H., Tovar,K., Baer,G., May,R.P., Hillen,W. and Heumann,H. (1989) The quaternary structure of Tet repressors bound to the Tn10-encoded tet gene control region determined by neutron solution scattering. *EMBO J.*, **8**, 1257–1263.
66. Merika,M., Williams,A.J., Chen,G., Collins,T. and Thanos,D. (1998) Recruitment of CBP/p300 by the IFN beta enhanceosome is required for synergistic activation of transcription. *Mol. Cell*, **1**, 277–287.
67. Giese,K., Kingsley,C., Kirshner,J.R. and Grosschedl,R. (1995) Assembly and function of a TCR alpha enhancer complex is dependent on LEF-1-induced DNA bending and multiple protein–protein interactions. *Genes Dev.*, **9**, 995–1008.
68. Mitta,B., Weber,C.C., Rimann,M. and Fussenegger,M. (2004) Design and *in vivo* characterization of self-inactivating human and non-human lentiviral expression vectors engineered for streptogramin-adjustable transgene expression. *Nucleic Acids Res.*, **32**, e106.
69. Fussenegger,M., Moser,S., Mazur,X. and Bailey,J.E. (1997) Autoregulated multicistronic expression vectors provide one-step cloning of regulated product gene expression in mammalian cells. *Biotechnol. Prog.*, **13**, 733–740.
70. Weber,W., Marty,R.R., Keller,B., Rimann,M., Kramer,B.P. and Fussenegger,M. (2002) Versatile macrolide-responsive mammalian expression vectors for multiregulated multigene metabolic engineering. *Biotechnol. Bioeng.*, **80**, 691–705.